Open access • Journal Article • DOI:10.1016/S1011-1344(99)00014-7

Systemic application of photosensitizers in the chick chorioallantoic membrane (CAM) model: photodynamic response of CAM vessels and 5-aminolevulinic acid uptake kinetics by transplantable tumors. — Source link

Rene Hornung, Marie J. Hammer-Wilson, Sol Kimel, Lih-Huei L. Liaw ...+2 more authors

Institutions: University of California, Irvine

Published on: 01 Mar 1999 - Journal of Photochemistry and Photobiology B-biology (Elsevier)

Topics: Photosensitizer, Photodynamic therapy and Protoporphyrin IX

Title
Systemic application of photosensitizers in the chick chorioallantoic membrane (CAM) model: photodynamic response of CAM vessels and 5-aminolevulinic acid uptake kinetics by transplantable tumors.

Journal
Journal of photochemistry and photobiology. B, Biology, 49(1)

ISSN
1011-1344

Authors
Hornung, R
Hammer-Wilson, MJ
Kimel, S
et al.

Publication Date
1999-03-01

DOI
10.1016/s1011-1344(99)00014-7

ELSEVIER

J. Photochem. Photobiol. B: Biol. 49 (1999) 41–49

Journal of Photochemistry and Photobiology B:Biology

Systemic application of photosensitizers in the chick chorioallantoic membrane (CAM) model: photodynamic response of CAM vessels and 5-aminolevulinic acid uptake kinetics by transplantable tumors

Rene Hornung [1], Marie J. Hammer-Wilson, Sol Kimel [2], Lih-Huei Liaw, Yona Tadir, Michael W. Berns *

Beckman Laser Institute and Medical Clinic, University of California, Irvine, Irvine, CA, USA

Received 10 July 1998; accepted 15 January 1999

Abstract

The aim of this study is to modify the chick chorioallantoic membrane (CAM) model into a whole-animal tumor model for photodynamic therapy (PDT). By using intraperitoneal (IP) photosensitizer injection of the chick embryo, use of the CAM for PDT has been extended to include systemic delivery as well as topical application of photosensitizers. The model has been tested for its capability to mimic an animal tumor model and to serve for PDT studies by measuring drug fluorescence and PDT-induced effects. Three second-generation photosensitizers have been tested for their ability to produce photodynamic response in the chick embryo/CAM system when delivered by IP injection: 5-aminolevulinic acid (ALA), benzoporphyrin derivative monoacid ring A (BPD-MA), and Lutetium-texaphyrin (Lu-Tex). Exposure of the CAM vasculature to the appropriate laser light results in light-dose-dependent vascular damage with all three compounds. Localization of ALA following IP injections in embryos, whose CAMs have been implanted with rat ovarian cancer cells to produce nodules, is determined in real time by fluorescence of the photoactive metabolite protoporphyrin IX (PpIX). Dose-dependent fluorescence in the normal CAM vasculature and the tumor implants confirms the uptake of ALA from the peritoneum, systemic circulation of the drug, and its conversion to PpIX.

Keywords: Chick chorioallantoic membrane; Rat ovarian cancer; Second-generation photosensitizers; Photodynamic therapy; Laser-induced fluorescence diagnostics

1. Introduction

Photodynamic therapy (PDT) depends on the differential uptake and retention of light-sensitive compounds in tumor tissue. Exposure to therapeutic light, at a wavelength selected to coincide with an absorption peak of the photosensitizer, results in oxidation-mediated destruction of the tumor mass and its supporting vasculature with minimal damage to the surrounding normal tissues [1–4]. Laser-induced fluorescence diagnostics (LIFD) uses photosensitizer-mediated fluorescence, allowing clinically relevant detection and treatment of malignant and premalignant lesions [4–12].

Animal models, such as rodents [13–35], rabbits [36], dogs [37,38], and primates [39,40] have been used in PDT and LIFD experiments. Specialized skinfold chambers even make it possible to visualize directly small tumors and their surrounding vasculature during experimentation [19,20]. However, most in vivo experiments are expensive, time consuming, and require long data-acquisition times. The chick embryo chorioallantoic membrane (CAM) model uses the well-vascularized chorioallantoic membrane of fertilized chicken eggs and presents an attractive in vivo model. It is inexpensive, allows direct visualization and video documentation of blood vessels, is easy to handle, and statistically useful numbers are attainable relatively quickly. The CAM system has been used to study both the growth and neovascularization of a wide variety of implanted tumor nodules or tumor cell suspensions [41–45]. Despite the ease of visualization of the tumors and their vascularization when grown on the CAM, the model has been used mainly to study PDT-induced injury of normal CAM vessels [46–49] and less for

* Corresponding author. Tel.: +1-949-824-6291; Fax: +1-949-824-8413; E-mail: mberns@bli.uci.edu

[1] Present address: Department of Obstetrics and Gynecology, University Hospital, Zürich, Switzerland.

[2] Permanent address: Department of Chemistry, Technion-Israel Institute of Technology, Haifa 32000, Israel.

1011-1344/99/$ - see front matter
PII S1011-1344(99)00014-7

PDT-induced necrosis of tumors growing on the CAM [49,50]. This is due, in part, to the difficulty of effectively delivering the photosensitizer to the tumor. Intravenous (IV) injection of the chick embryo CAM is possible [51–53], but the time needed for injection of the large numbers of eggs required per experiment is prohibitive and the success rate is comparatively low. Yolk sac injection works for some but not all compounds [49,54]. Topical application is simple but of interest mainly for studies related to surface-accessible lesions or dermatological conditions. The intraperitoneal (IP) injection method of delivery used in our study more closely approximates the IV delivery most commonly used in mammalian models, since photosensitizers reach the CAM vessels through the circulatory system of the embryo.

The aims of this study were two-fold: (1) to demonstrate the feasibility and usefulness of systemic photosensitizer administration to the CAM model for PDT studies by showing that the CAM vasculature is a photodynamic target of the circulating photosensitizer; (2) to demonstrate the feasibility of using IP injected chick embryos and their CAM systems for LIFD studies by measuring the localization of a fluorescent compound over time in an implanted tumor.

2. Materials and methods

2.1. CAM preparation

The CAM model has been described previously [46,47,49,55] and was used here with minor modifications. Briefly, fertilized chicken eggs were disinfected and transferred to a hatching incubator set at 38°C and 60% humidity, and equipped with an automatic rotator (Profi I, Lyon Electric, Chula Vista, CA). On the fourth day of embryo development (EDD 4), 4–5 ml of albumin was aspired with a syringe connected to a 20 gauge needle, through a hole drilled at the narrow apex, to create a false air sac. On EDD 7, a 20 mm diameter hole was cut into the shell and covered with a sterile Petri dish. Egg incubation was continued in a static incubator.

The CAM consists of a superficial two-dimensional structure composed of three layers: an external layer of epithelial cells derived from the chorion ectoderm, an intermediate layer of mesoderm derived from the fusion of the chorionic and allantoic mesoderms, and an internal layer of epithelial cells derived from the allantoic endoderm [55,56]. The mesodermal layer contains the extraembryonic vascular network, which is supplied by two primary arteries and drained by a single vein from the embryo [56]. Precapillary (arteriole) and postcapillary (venule) blood vessels are characterized by their size [55–57]. Order-I vessels describe the smallest visible vessels (diameter ~50 μm); the convergence of two order-I vessels is assigned as an order-II vessel (diameter ~70 μm); similarly, two order-II vessels form an order-III vessel (diameter ~110 μm).

2.2. Cell culture

The NuTu-19 cell line is a poorly differentiated epithelial ovarian cancer cell line that spontaneously developed in the Fischer 344 rat [58,59]. Tissue-culture-adapted NuTu-19 cells were grown in RPMI 1640 medium supplemented with 10% fetal bovine serum (Life Technologies, Grand Island, NY), 25 IU/ml penicillin and 25 mg/ml streptomycin. Flasks were maintained in a 37°C incubator with 7.5% CO_2 and 100% humidity. Subculture was done weekly using enzyme release and a 1:10 dilution in fresh medium.

2.3. Cell implantation

NuTu-19 cells were harvested by washing the flask with Ca^{2+}, Mg^{2+}-free PBS, followed by treatment with a mixture of 0.125% trypsin, 0.625 g/ml Pancreatin (Life Technologies, Grand Island, NY) and 0.05% EDTA. The released sheets of cells were pipetted to break the cells further apart and the resulting suspension was centrifuged to remove the enzyme. The cells were resuspended in fresh medium, passed through an 18 gauge needle and the concentration of the resulting suspension (cells/ml) was determined using a hemocytometer. Additional medium was added as needed to give a final concentration of 200×10^6 cells/ml.

On EDD 8, aliquots of cells were placed on CAMs which had been prepared by a modified combination of the techniques of Preminger et al. [43] and Petruzzelli et al. [44]. A 6 mm inner diameter Teflon ring was placed on the CAM centered over a Y branch of an order-II vessel demarcating an area of 28 mm^2. The ectodermal epithelium of the demarcated area was then abraded using a 30 gauge hypodermic needle. The debris and exudate were gently aspirated from the newly exposed mesodermal layer. A 25 μl sample containing 5×10^6 NuTu-19 cells was placed in the center of the 'opened' surface. The eggs were sealed with Parafilm® (American National Can, Neewah, WI) and returned to the incubator until the tumors were of sufficient size for experimentation (EDD 12/13).

2.4. Histology

On EDD 12/13 representative tumors were selected for histological evaluation to confirm vascularization. Specimens were fixed in 10% formalin, dehydrated in a graded alcohol series, and embedded in paraffin. Serial sections 6 μm thick were cut on a rotary microtome and stained with Hematoxylin and Eosin. The slides were examined at 250× using an Olympus BH-2 microscope (Olympus, Japan).

2.5. Photosensitizers

5-aminolevulinic acid (ALA, DUSA Pharmaceuticals, Denville, NJ) solutions of 10, 25, 50, or 100 mg/ml in H_2O (adjusted to pH ~6 with NaOH) were freshly prepared before each experiment.

The liposomal powder of benzoporphyrin derivative monoacid ring A (BPD-MA, QLT, Vancouver) was reconstituted in sterile water according to the manufacturer's directions to give a final concentration of 2 mg/ml.

Lutetium texaphyrin (Lu-Tex, Compound PCI-0123, Pharmacyclics, Sunnyvale, CA), a powdered compound, was dissolved in 5% mannitol to give a final concentration of 2 mg/ml.

Both ALA and Lu-Tex were filter sterilized before injection into the embryos. BPD-MA was prepared sterilely according to the manufacturer's directions.

2.6. Laser systems and irradiation parameters for PDT

Wavelengths for irradiation were 635 nm (for ALA), 690 nm (for BPD-MA), and 740 nm (for Lu-Tex). Continuous-wave radiation at 635 nm was delivered by an argon laser pumped dye laser (model CR599, Coherent, Palo Alto, CA) and at 690 or 740 nm by microchannel cooled stacked diode lasers (Lawrence Livermore Laboratories, Livermore, CA). Light was transmitted through a 400 μm multimode fiber terminated with a microlens (PDT Systems, Santa Barbara, CA). The beam was expanded to a spot 8.8 mm in diameter to cover the entire area demarcated by a Teflon ring with a 6 mm inner diameter and 1.4 mm wide annulus (60 mm^2). Laser output was measured using a Coherent model 210 power meter. Eggs without photosensitizer were irradiated at each wavelength to determine the radiant exposure at which light-induced damage occurred. All irradiation conditions were well below these levels. The intensity was 100 mW/cm^2; irradiation times were 50, 100, or 200 s, yielding irradiances of 5, 10, and 20 J/cm^2, respectively, corresponding to energies incident within the open ring area (28 mm^2) of 1.5, 3, and 6 J.

2.7. Vascular PDT and damage assessment

Non-tumor-bearing eggs at EDD 12 or EDD 13 were used to determine the photodynamic damage induced in the normal CAM vasculature after IP injection of photosensitizer. Based on the mean weight estimates for embryos of these ages [60], embryos were injected with either 30 μl (EDD 12, embryo weight ~10 g) or 40 μl (EDD 13, embryo weight ~13 g) of photosensitizer solution using a 2.5 cm 30 gauge needle attached to a 250 μl Hamilton syringe. Approximate dosages were ALA 75 mg/kg, BPD 6 mg/kg, and Lu-Tex 6 mg/kg. After injection, a 6 mm inner diameter Teflon ring was placed on the CAM surface. The eggs were covered with a blackened Petri dish and returned to the incubator. After 90 min, individual eggs were removed and the ring area exposed to 1.5, 3, or 6 J laser light of the appropriate wavelength. Following irradiation, the eggs were returned to the incubator for an additional 60 min.

Damage was observed using a Wild stereomicroscope (model M5, Wild Heerbrugg, Switzerland) at a final magnification of 250×. Movement of the blood through the vessels was easily visualized at this magnification. Each egg was graded in a double blind fashion according to the highest degree of damage observed within the irradiated area. The damage scale used was a modification of that described previously [46,47,49,57]: 0, no observable damage; 0.5, capillary hemorrhage only; 1, stasis in order-I vessels or temporary occlusion of order-II vessels; 2, stasis in order-II vessels or hemorrhage of order-I vessels; 3, stasis in order-III vessels or hemorrhage of order-II vessels. Seven to ten eggs were evaluated for each sensitizer–light-dosage combination. Results are presented as the mean ± standard error of the mean (SEM).

2.8. Fluorescence data acquisition

Tumor-bearing eggs at EDD 12–14 (i.e., four to six days after cell implantation) were used to determine the time course of the appearance of fluorescence in the tumor nodule and the surrounding vasculature. The eggs were placed in a heating block filled with glass beads (Isotemp Dry Bath 147, Fisher Scientific, Pittsburgh, PA) under the imaging CCD camera. Tumor baseline fluorescence was determined three times at 1 min intervals prior to photosensitization. Without moving the egg, ALA was injected IP into the embryo. Immediately after injection and for 2 h afterwards (at 5 min intervals) ALA-mediated fluorescence was measured.

Low-light-level fluorescence imaging was performed with a slow scan, thermoelectrically cooled CCD camera with 16 bit/pixel dynamic range (TECCD-576E/UV, Princeton Instruments, Trenton, NJ) equipped with a Nikon objective (Nikkor 50 mm, 1:1.2, Nikon, Melville, NY) and a 650 nm long-bandpass filter (FWHM 25 nm; Corion, Holliston, MA). Fluorescence excitation was provided by an Ar-ion laser (Innova 90-5, Coherent, Palo Alto, CA) tuned to 514 nm. Exposure time was 20 ms. The wavelength was verified with a Hartridge Reversion Spectroscope (Ealing Electro-Optics, South Natick, MA). The laser beam passed through a mechanical shutter (UniBlitz model T 132, Vincent Associates, Rochester, NY) and an optical fiber with a front light diffuser onto the specimen. The final output power was adjusted to 400 mW, as measured with a power meter (model 210, Coherent, Palo Alto, CA). The intensity at the illumination spot was 175 mW/cm^2, providing an irradiance of 0.0035 J/cm^2, a level unlikely to cause PDT effects. Instrument control, image acquisition, and processing were performed with IPlab software (Signal Analytic, Vienna, VA).

2.9. Fluorescence evolution analysis

Baseline fluorescence intensities were averaged and defined as the tumor autofluorescence. ALA-mediated fluorescence of the tumor nodules at selected time points following drug administration was divided by the tumor autofluorescence to determine the relative changes in fluorescence. For each ALA dose, relative fluorescence intensities of three tumors were measured. Data are presented as the

mean values at each time point for each drug dosage with linear regression lines drawn for each data set. Similar calculations were done for the vessels surrounding the tumors using the autofluorescence of the vessels as the baseline. Probability values comparing the fluorescence of the vessels to that of the tumors at $t = 120$ min (the time of maximum difference) were calculated using Student's t-test.

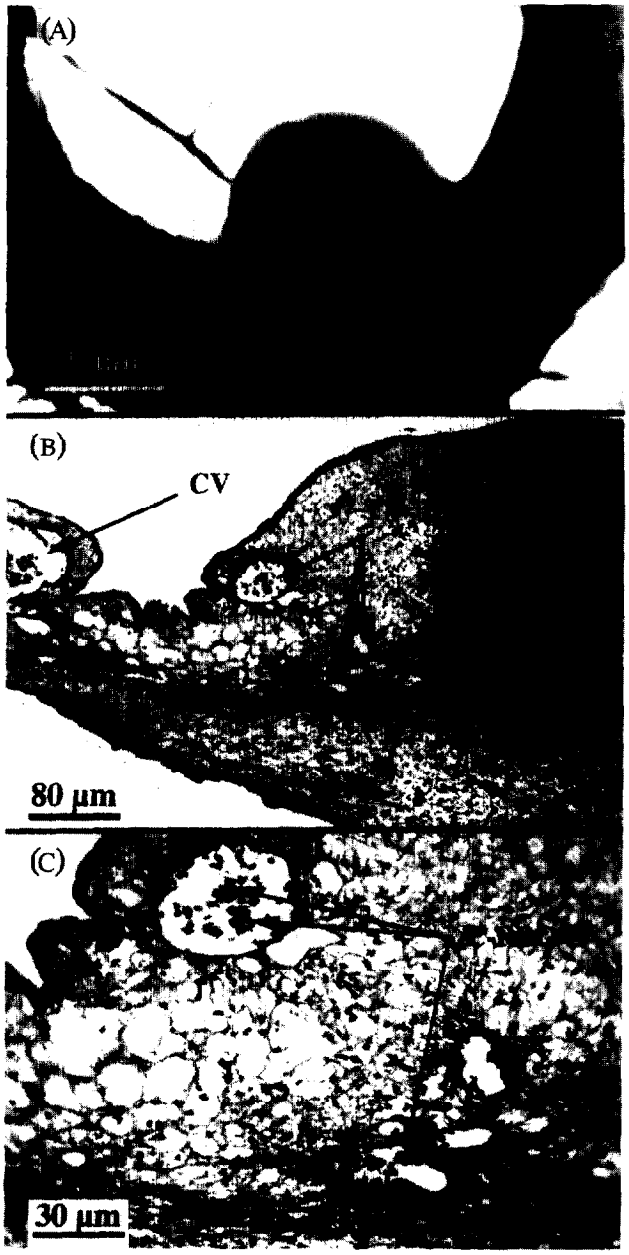

Fig. 1. NuTu-19 tumor after 5 days' growth on the CAM. (A) Stereomicrograph of an excised portion of the CAM showing a tumor in situ. The tumor-bearing CAM has been inverted to allow visualization of the vessels on the undersurface of the tumor nodule. (B) Histologic section of the nodule in (A) confirming the internal vascularization of the cell mass: CV = CAM vessel, TV = tumor-surrounded vessel. Hematoxylin and Eosin stain. (C) Higher-magnification view of tumor vessel area in (B) showing nucleated chicken red blood cells (C-RBC) contained within the vessel lumen. Hematoxylin and Eosin stain.

3. Results

3.1. Cell implantation

Although cell implantation of the CAM is technically possible by EDD 5 [41], we found that EDD 8 provided the optimal conditions. The CAM was sufficiently developed to support the Teflon ring (with minimal shifting of location), the still-developing vasculature [55,56] provided better infiltration of the forming tumor nodule, and we had a larger 'window' of time over which the system could be used. Creating a depression by opening the surface kept the cells more localized and allowed closer proximity between the cells and the underlying vasculature, thus facilitating vessel growth into the cell mass. Within two days of seeding (EDD 10), the upper epithelial layer of the CAM had 'healed' over the tumor cells, encapsulating them. By four days post-seeding (EDD 12), vessels were visible on the tumor surface (Fig. 1(A)). All vessels within the tumor mass were perfused with nucleated erythrocytes characteristic for avian species, proving that the neovascularization of the tumor was connected to the chick's circulation system (Fig. 1(B) and (C)). Using this method, rather than the method of dropping cells on the intact CAM surface [49,58], we were able to achieve an approximately 80% yield of usable tumors of the CAMs implanted.

3.2. Injury of normal vessels

Fig. 2 exhibits the degree of photodynamic damage induced in the normal CAM vasculature for each of the photosensitizers after 90 min uptake. As expected [4,16, 29,30,40], all compounds showed an increase in damage with increasing light dosage. Both BPD-MA and ALA appear to have reached a maximum with 3 J. With Lu-Tex the injury continued to increase linearly over the entire light-dose range tested.

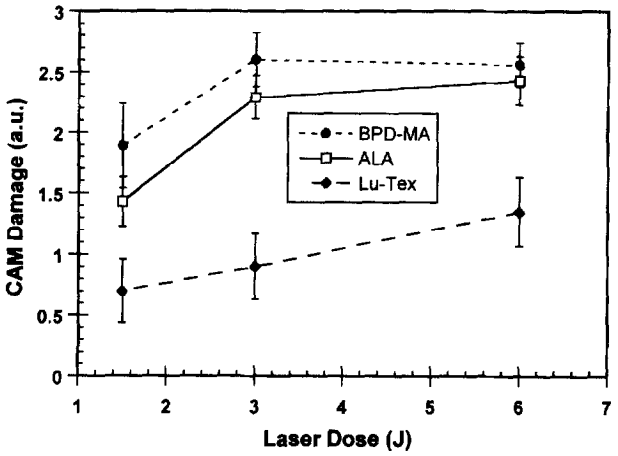

Fig. 2. Vascular damage (arbitrary scoring system, see text) induced in normal vessels of the CAM when irradiated with laser light 90 min after IP injection of the chick embryo with 75 mg/kg ALA, 6 mg/kg BPD-MA, or 6 mg/kg Lu-Tex. Each data point is the mean of 7–10 eggs ± SEM.

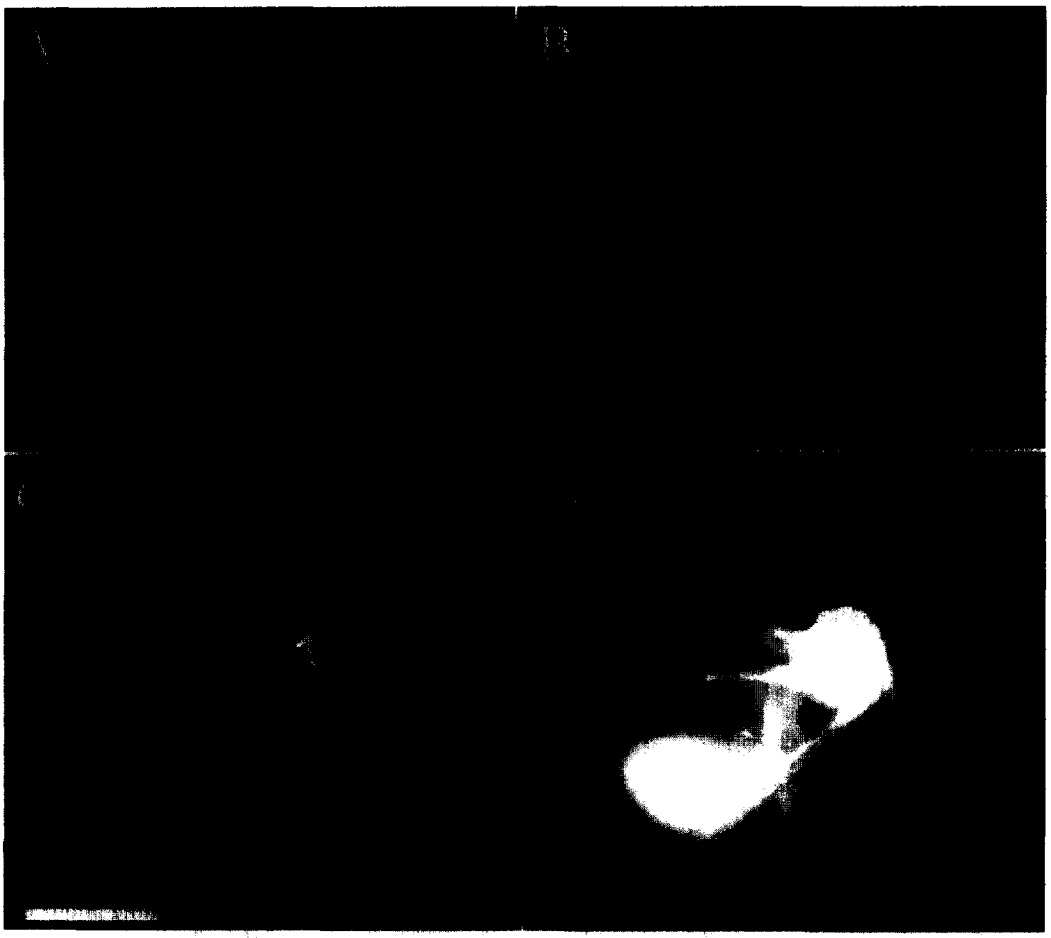

Fig. 3. Time-dependent increase in vascular and tumor fluorescence seen after IP injection of the chick embryo with 150 mg/kg ALA: (A) 1 min pre-injection; (B) 30 min post-injection; (C) 60 min post-injection; (D) 120 min post-injection.

3.3. Tumor and vascular fluorescence

Fig. 3 shows a typical NuTu-19 tumor and its surrounding vasculature at 1 min prior to ALA injection (A), and at 30 min (B), 60 min (C), and 120 min post-injection (D). Clearly, there is a time-dependent increase in the fluorescence intensity of these structures.

Fig. 4 shows relative fluorescence (measured fluorescence intensity divided by the autofluorescence) for the tumors and their surrounding vessels as a function of time (minutes) following intraperitoneal injection of 10 mg/ml (30 mg/kg) and 50 mg/ml (150 mg/kg) ALA. Five to ten minutes following injection, the fluorescence of vessels and tumors started to increase. Both doses used for this study showed a first-order linear increase of fluorescence with time over the observation period of 2 h. In the tumors, 2 h after IP administration, 30 mg/kg ALA reached fluorescence levels 1.5-fold higher than autofluorescence, whereas for 150 mg/kg ALA the ratio was 25. A similar behavior was observed for the vessel fluorescence: 30 mg/kg caused a 3-fold increase and 150 mg/kg a ratio of 30. In contrast, 300 mg/kg ALA did not show higher fluorescence levels than 150 mg/kg ALA (data not shown). At the early times, vessels and tumors display about the same increase in fluorescence. By 2 h post-injection, the fluorescence in the vessels is greater than that in the tumors but not significantly for either concentration ($p_{30}=0.06$, $p_{150}=0.47$). This most likely represents a high

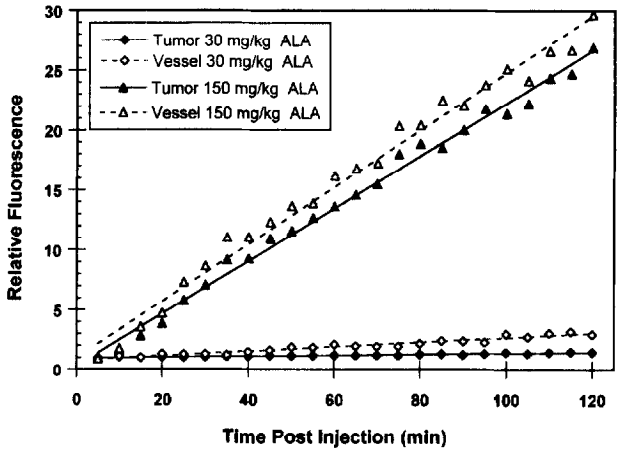

Fig. 4. Increase in relative fluorescence (measured fluorescence/autofluorescence) in NuTu-19 tumors growing on the CAM and their surrounding vasculature following IP injection of the chick embryo with 30 and 150 mg/kg ALA. Each data point is the mean of three eggs. Linear regression lines have been drawn for each tissue type at each ALA concentration. The R^2 values for each are $\text{Tumor}_{150}=0.417$, $\text{Vessel}_{150}=0.426$, $\text{Tumor}_{30}=0.729$, $\text{Vessel}_{30}=0.701$.

concentration of PpIX in the red blood cells as well as in the vessel walls [51].

4. Discussion

PDT is currently being evaluated as an adjuvant to surgery, radiotherapy, and chemotherapy for the treatment of malignant tumors. The rapid development of PDT and of LIFD requires an experimental setup that allows fast assessment of their technologies. Novel photosensitizers, light sources, and light diffusers have to be effectively evaluated. It is known that the biology of cancer varies from tumor to tumor and from patient to patient. Thus there is a need for an in vivo assay allowing rapid assessment of tumor response to PDT in order to determine optimal PDT parameters on an individual patient basis.

Recent studies utilizing the CAM system have measured real-time fluorescence following topical [47,51], yolk sac [49], or IV [51,52] administration of photosensitizers. In situ, real-time measurements of fluorescence have also been made on the CAM to demonstrate the effects of modulators on PpIX production following topical application of ALA [50]. However, the overall clinical relevance of studies where photosensitizers are topically applied or injected into the yolk sac is questionable.

The primary disadvantage of the CAM as a PDT model has been its limitation to topical sensitization. Except for surface tumors, PDT animal models use systemic delivery (IV, IP or oral) of the photosensitizer to the tumor site. Intravenous injection is used most frequently [18–33,36–40], although a number of studies used IP injection [13–17]. Oral [23,35] and topical [34,35] administration are used infrequently. Our study examined the feasibility of using IP injection of the chick embryo as a method of achieving systemic photosensitizer delivery that allows evaluation of uptake kinetics in tumors growing on the CAM and of PDT responses in the CAM vasculature.

Our data clearly demonstrate that IP administration of ALA is followed by rapid uptake by the peritoneum as well as fast conversion of ALA to PpIX. Using IP-administered ALA, the nonfluorescent metabolic precursor of PpIX, we were able to detect a dose-dependent increase in vascular and tumor fluorescence over time. This demonstrates that ALA was absorbed by the peritoneum, passed into the circulatory system, and was metabolized into the fluorescent metabolite PpIX at a location different from its delivery point. The data suggest that 30 mg/kg ALA represents the lowest dose that can be reliably detected with our setup. In addition, it appears that the system consisting of embryo, CAM, and tumor is not capable of metabolizing more than 150 mg/kg ALA. Maximum fluorescence was seen at concentrations near those where photodynamic effects are observed in mammalian systems [13–15,20–25,35] and human subjects [4,6,9–11]. In mice with lung adenomas [13], using ALA dosages comparable to ours, the uptake time course and fluorescence increase were similar to those found in the CAM/tumor system. In mice with colon carcinoma [14], using ALA at dosages lower than we could detect, uptake peaked sooner (at 1 h) with a low relative fluorescence increase (2.3 times). This may simply reflect complete metabolism of the ALA delivered rather than a maximal obtainable value, which is what we appear to have achieved. The observation by Loh et al. [23] that in the rat lower doses of ALA reach peak fluorescence before higher doses would support this explanation. Also, other investigators [36,38] have reported shifts in peak times for maximal PpIX concentration in blood that were dose dependent, i.e., higher doses peaked at later times. In other mammalian studies, maximal fluorescence times ranged between 30 min and 4 h [14,15,19–24,27,37]. The variation in peak fluorescence times found in the above studies may be explained by the different rates of PpIX production in the cell types examined [61]. Clearly the embryo/CAM/tumor system produces measurable fluorescence within the same time frame as these other more complex systems.

Our aim in assaying PDT damage in the normal vasculature was two-fold. First, we wanted to compare photosensitizers injected IP in different formulations and, presumably, delivered to tissue via different routes. ALA requires metabolization to produce the photosensitizing agent PpIX [4], Lu-Tex represents a water-soluble compound [16,30], whereas BPD-MA is administered encapsulated in liposomes [29,40]. Since we deliberately chose high concentrations of the test compounds, in order to maximize the possibility of fluorescence detection of circulating photosensitizer, it is not surprising that with high radiant exposures we appear to have reached the upper limit (damage level 3) of the system under the conditions tested for ALA and BPD-MA. Use of lower ALA and BPD-MA dosages, or lower radiant exposures, would most probably have resulted in linear damage effects over the energy range tested, as was obtained for Lu-Tex. Secondly, we hoped to confirm that the appearance of tumor fluorescence correlated with the time when vascular damage could be produced. Both objectives were achieved. All three sensitizers, regardless of formulation, entered the circulatory system such that exposure to radiation at the appropriate wavelength elicited vascular damage. ALA, at 90 min post-injection, showed increased tumor fluorescence as well as induction of vascular damage. Although we tested only ALA for correlation of fluorescence with PDT, it should be possible to perform similar measurements with the CCD camera system modified to match the excitation/emission wavelengths of other photosensitizers.

Historically, tissue distribution and pharmacokinetic studies of photosensitizers have been based on empirical observations of PDT effects [21,25,32], fluorescence analysis of frozen tissue sections [11,13,25–27,31], quantitation of photosensitizer extracted from tissue samples [21,26,28,31], or measurement of radiolabeled sensitizer retained by the target and other tissues [29,33,34]. Fluorescence measurements of living tissue have been used primarily for the localization of tumors, after optimal uptake times had been previously estab-

lished [4,6,12]. Fluorescence measurements to establish time courses in whole animals have been limited to surface (skin) measurements [8,14,15,17] or skinfold chamber observations [19,20]. The chick embryo/CAM system permits real-time visualization of the uptake and distribution of photosensitizers in a vascularized tumor model using fluorescence monitoring. Correlation of PDT effects with the fluorescence evolution profile can be verified using the damage inflicted when the CAM vasculature and/or tumor nodule are irradiated. IP injection of the chick embryo provides a method of photosensitizer delivery that allows easy handling of the large number of CAMs needed to evaluate meaningfully uptake kinetics and PDT responses. This system provides a bridge between studies done at the cellular level in tissue culture and whole-animal mammalian models. A potential clinical application for the CAM system may be PDT sensitivity testing for a variety of different tumors, since any tumor type that can be grown on the CAM can be investigated. In the future, it may be possible to predict a patient's tumor responses prior to PDT treatment using the CAM system. Such testing would be useful for individualized optimization of PDT parameters instead of applying a standard 'one protocol fits all' to every patient. Another possible clinical application would be the testing of new fluorescence devices, such as cystoscopes, laparoscopes, or other endoscopes, by placing the CAM system in a suitable enclosure to mimic various body cavities.

5. Conclusions

We have demonstrated that the technique of injection of photosensitizer into the peritoneal cavity of the chick embryo transforms the CAM system into a whole-animal model which is suitable for rapid, inexpensive testing of PDT and LIFD technologies. We have also developed a modified method of producing tumor growth on the CAM which should increase its usefulness for future studies of tumors and their supporting vasculature.

Acknowledgements

This research was supported by NIH Contract grants 2RO1CA32248 and RRO1192, DOE Contract grant DE-FG03-91ER61227, US–Israel Binational Science Foundation grant 93-00154, and Schweizerischer Nationalfonds zur Foerderung wissenschaftlicher Forschung. The authors thank J. Andrews for assistance with the lasers, H. Li for maintenance of cell cultures, D. Chavez, J. Eusebio, and D. Cao for help with CAM preparation, T.B. Krasieva for photomicrograph assembly, and A. Iannucci for statistical assistance. We also thank DUSA, QLT, and Pharmacyclics for supplying us with the photosensitizers used in this study.

References

[1] A.M.R. Fisher, A.L. Murphree, C.J. Gomer, Clinical and preclinical photodynamic therapy, Lasers Surg. Med. 17 (1995) 2–31.
[2] B.W. Henderson, T.J. Dougherty, How does photodynamic therapy work?, Photochem. Photobiol. 55 (1992) 145–157.
[3] T.J. Dougherty, Photodynamic therapy, Photochem. Photobiol. 58 (1993) 895–900.
[4] Q. Peng, T. Warloe, K. Berg, J. Moan, M. Kongshaug, K.E. Giercksky, J.M. Nesland, 5-Aminolevulinic acid-based photodynamic therapy. Clinical research and future challenges, Cancer 79 (1997) 2282–2308.
[5] G.A. Wagnières, W.M. Star, B.C. Wilson, In vivo fluorescence spectroscopy and imaging for oncological applications, Photochem. Photobiol. 68 (1998) 603–632.
[6] S.L. Marcus, R.S. Sobel, A.L. Golub, R.L. Carol, S. Lundahl, D.G. Shulman, Photodynamic therapy (PDT) and photodiagnosis (PD) using endogenous photosensitization induced by 5-aminolevulinic acid (ALA): current clinical and development status, J. Clin. Laser Med. Surg. 79 (1996) 59–66.
[7] W.D. Tope, E.V. Ross, N. Kollias, A. Martin, R. Gillies, R.R. Anderson, Protoporphyrin IX fluorescence induced in basal cell carcinoma by oral δ-aminolevulinic acid, Photochem. Photobiol. 67 (1998) 249–255.
[8] A. Orenstein, G. Kostenich, Z. Malik, The kinetics of protoporphyrin fluorescence during ALA-PDT in human malignant skin tumors, Cancer Lett. 120 (1997) 229–234.
[9] J. Webber, D. Kessel, D. Fromm, On-line fluorescence of human tissues after oral administration of 5-aminolevulinic acid, J. Photochem. Photobiol. B: Biol. 38 (1997) 209–214.
[10] K.F. Fan, C. Hopper, P.M. Speight, G. Buonaccorsi, A.J. MacRobert, S.G. Bown, Photodynamic therapy using 5-aminolevulinic acid for premalignant and malignant lesions of the oral cavity, Cancer 78 (1996) 1374–1383.
[11] P. Mlkvy, H. Messmann, J. Regula, M. Conio, M. Pauer, C.E. Millson, A. MacRobert, S.G. Bown, Sensitization and photodynamic therapy (PDT) of gastrointestinal tumors with 5-aminolevulinic acid (ALA) induced protoporphyrin IX (PPIX). A pilot study, Neoplasma 42 (1995) 109–113.
[12] S. Andersson-Engels, C. Klinteberg, K. Svanberg, S. Svanberg, In vivo fluorescence imaging for tissue diagnostics, Phys. Med. Biol. 42 (1997) 815–824.
[13] D.L. Campbell, E.F. Gudgin-Dickson, P.G. Forkert, R.H. Pottier, J.C. Kennedy, Detection of early stages of carcinogenesis in adenomas of murine lung by 5-aminolevulinic acid-induced protoporphyrin IX fluorescence, Photochem. Photobiol. 64 (1996) 676–682.
[14] A. Orenstein, G. Kostenich, L. Roitman, Y. Shechtman, Y. Kopolovic, B. Ehrenberg, Z. Malik, Comparative study of tissue distribution and photodynamic therapy selectivity of chlorin e6, Photofrin II and ALA-induced protoporphyrin IX in a colon carcinoma model, Br. J. Cancer 73 (1996) 937–944.
[15] N. van der Veen, H.S. de Bruijn, R.J. Berg, W.M. Star, Kinetics and localization of PpIX fluorescence after topical and systemic ALA application, observed in skin and skin tumours of UVB-treated mice, Br. J. Cancer 73 (1996) 925–930.
[16] G. Kostenich, A. Orenstein, L. Roitman, Z. Malik, B. Ehrenberg, In vivo photodynamic therapy with the new near-IR absorbing water soluble photosensitizer lutetium texaphyrin and a high intensity pulsed light delivery system, J. Photochem. Photobiol. B: Biol. 39 (1997) 36–42.
[17] J.C. Kennedy, P. Nadeau, J. Petryka, R.H. Pottier, G. Weagle, Clearance times of porphyrin derivatives from mice as measured by in vivo fluorescence spectroscopy, Photochem. Photobiol. 55 (1992) 729–734.
[18] S. Andersson-Engels, J. Ankerst, J. Johansson, K. Svanberg, S. Svanberg, Laser-induced fluorescence in malignant and normal tissue

of rats injected with benzoporphyrin derivative, Photochem. Photobiol. 57 (1993) 978–983.

[19] C. Abels, P. Heil, M. Dellian, G.E. Kuhnle, R. Baumgartner, A.E. Goetz, In vivo kinetics and spectra of 5-aminolaevulinic acid-induced fluorescence in an amelanotic melanoma of the hamster, Br. J. Cancer 70 (1994) 826–833.

[20] N. van der Veen, H.L. van Leengoed, W.M. Star, In vivo fluorescence kinetics and photodynamic therapy using 5-aminolaevulinic acid-induced porphyrin: increased damage after multiple irradiations, Br. J. Cancer 70 (1994) 867–872.

[21] J. Bedwell, A.J. MacRobert, D. Phillips, S.G. Bown, Fluorescence distribution and photodynamic effect of ALA-induced PP IX in the DMH rat colonic tumour model, Br. J. Cancer 65 (1992) 818–824.

[22] S. Iinuma, R. Bachor, T. Flotte, T. Hasan, Biodistribution and phototoxicity of 5-aminolevulinic acid-induced PpIX in an orthotopic rat bladder tumor model, J. Urol. 153 (1995) 802–806.

[23] C.S. Loh, A.J. MacRobert, J. Bedwell, J. Regula, N. Krasner, S.G. Bown, Oral versus intravenous administration of 5-aminolaevulinic acid for photodynamic therapy, Br. J. Cancer 68 (1993) 41–51.

[24] J. Johansson, R. Berg, K. Svanberg, S. Svanberg, Laser-induced fluorescence studies of normal and malignant tumour tissue of rat following intravenous injection of delta-aminolevulinic acid, Lasers Surg. Med. 20 (1997) 272–279.

[25] F. Cairnduff, D.J. Roberts, B. Dixon, S.B. Brown, Response of a rodent fibrosarcoma to photodynamic therapy using 5-aminolaevulinic acid or polyhaematoporphyrin, Int. J. Radiat. Biol. 67 (1995) 93–99.

[26] P.T. Chatlani, P.J.O. Nuutinen, N. Toda, H. Barr, A.J. MacRobert, J. Bedwell, S.G. Bown, Selective necrosis in hamster pancreatic tumours using photodynamic therapy with phthalocyanine photosensitization, Br. J. Surg. 79 (1992) 786–790.

[27] S. Gronlund-Pakkanen, K. Makinen, M. Talja, A. Kuusisto, E. Alhava, The importance of fluorescence distribution and kinetics of ALA-induced PpIX in the bladder in photodynamic therapy, J. Photochem. Photobiol. B: Biol. 38 (1997) 269–273.

[28] C. Abels, C. Fritsch, K. Bolsen, R.M. Szeimies, T. Ruzicka, G. Goerz, A.E. Goetz, Photodynamic therapy with 5-aminolaevulinic acid-induced porphyrins of an amelanotic melanoma in vivo, J. Photochem. Photobiol. B: Biol. 40 (1997) 76–83.

[29] A.M. Richter, E. Waterfield, A.K. Jain, A.J. Canaan, B.A. Allison, J.G. Levy, Liopsomal delivery of a photosensitizer benzoporphyrin derivative monoacid ring A (BPD), to tumor tissue in a mouse tumor model, Photochem. Photobiol. 57 (1993) 1000–1006.

[30] K.W. Woodburn, Q. Fan, D.R. Miles, D. Kessel, Y. Luo, S.W. Young, Localization and efficacy analysis of the phototherapeutic lutetium texaphyrin (PCI-0123) in the murine EMT6 sarcoma model, Photochem. Photobiol. 65 (1997) 410–415.

[31] M.J. Witjes, A.J. Mank, O.C. Speelman, R. Posthumus, C.A. Nooren, J.M. Nauta, J.L. Roodenburg, W.M. Star, Distribution of aluminum phthalocyanine disulfonate in an oral squamous cell carcinoma model, in vivo fluorescence imaging compared with ex vivo analytical methods, Photochem. Photobiol. 65 (1997) 685–693.

[32] C.J. Gomer, A. Ferrario, Tissue distribution and photosensitizing properties of mono-L-aspartyl chlorin e6 in a mouse tumor model, Cancer Res. 50 (1990) 3985–3990.

[33] J. Rousseau, R. Langlois, H. Ali, J.E. van Lier, Biological activities in phthalocyanines XI: Synthesis, tumor uptake and biodistribution of ^{14}C-labeled disulfonated and trisulfonated gallium phthalocyanine in C3H mice, J. Photochem. Photobiol. B: Biol. 6 (1990) 121–132.

[34] R.A. Steiner, Y. Tadir, B.J. Tromberg, T. Krasieva, A.T. Gazains, P. Wyss, M.W. Berns, Photosensitization of the rat endometrium following 5-aminolevulinic acid induced photodynamic therapy, Lasers Surg. Med. 18 (1996) 301–308.

[35] S.C. Chang, G. Buonaccorsi, A.J. MacRobert, S.G. Bown, 5-Aminolevulinic acid (ALA)-induced protoporphyrin IX fluorescence and photodynamic affects in the rat bladder: an in vivo study comparing oral and intravesical ALA administration, Lasers Surg. Med. 20 (1997) 252–264.

[36] L.A. Lofgren, A.M. Ronn, M. Nouri, C.J. Lee, D. Yoo, B.M. Steinberg, Efficacy of intravenous δ-aminolevulinic acid photodynamic therapy on rabbit papillomas, Br. J. Cancer 72 (1995) 857–864.

[37] S.C. Chang, G.A. Buonaccorsi, A.J. MacRobert, S.G. Bown, Interstitial photodynamic therapy in the canine prostate with disulfonated aluminum phthalocyanine and 5-aminolevulinic acid-induced protoporphyrin IX, Prostate 32 (1997) 89–98.

[38] N.G. Egger, M. Motamedi, M. Pow-Sang, E. Orihuela, K.E. Anderson, Accumulation of porphyrins in plasma and tissues of dogs after δ-aminolevulinic acid administration: implications for photodynamic therapy, Pharmacology 52 (1996) 362–370.

[39] M.L. Pantelides, J.V. Moore, E. Forbes, T.G. Truscott, N.J. Blacklock, The uptake of porphyrin and zinc-metalloporphyrin by the primate prostate, Photochem. Photobiol. 57 (1993) 838–841.

[40] M. Kramer, J.W. Miller, N. Michaud, R.S. Moulton, T. Hasan, T.J. Flotte, E.S. Gragoudas, Liposomal benzoporphyrin derivative verteporfin photodynamic therapy. Selective treatment of choroidal neovascularization in monkeys, Ophthalmology 103 (1996) 427–438.

[41] D. Knighton, D. Ausprunk, D. Tapper, J. Folkman, Avascular and vascular phases of tumor growth in the chick embryo, Br. J. Cancer 35 (1977) 347–356.

[42] I. Ishiwata, C. Ishiwata, M. Soma, I. Ono, T. Nakaguchi, H. Ishikawa, Tumor angiogenic activity of gynecologic tumor cell lines on the chorioallantoic membrane, Gynecologic Oncology 29 (1988) 87–93.

[43] G.M. Preminger, W.F. Koch, F.A. Fried, J. Mandell, Chorioallantoic membrane grafting of the embryonic murine kidney. An improved in vitro technique for studying kidney morphogenesis, Invest. Urol. 18 (1981) 377–381.

[44] G.J. Petruzzelli, C.H. Snyderman, J.T. Johnson, E.N. Myers, Angiogenesis induced by head and neck squamous cell carcinoma xenografts in the chick embryo chorioallantoic membrane model, Ann. Otol. Rhinol. Laryngol. 102 (1993) 215–221.

[45] L.M. Kirchner, S.P. Schmidt, B.S. Gruber, Quantitation of angiogenesis in the chick chorioallantoic membrane model using fractal analysis, Microvascular Res. 51 (1996) 2–14.

[46] V. Gottfried, E.S. Lindenbaum, S. Kimel, Vascular damage during PDT as monitored in the chick chorioallantoic membrane, Int. J. Radiat. Biol. 60 (1991) 349–354.

[47] H. Toledano, R. Edrei, S. Kimel, Photodynamic damage by liposome-bound porphycenes: Comparison between in vitro and in vivo models, J. Photochem. Photobiol. B: Biol. 42 (1998) 20–27.

[48] W.S.L. Strauss, R. Sailer, H. Schneckenburger, N. Akguen, V. Gottfried, L. Chetwer, S. Kimel, Photodynamic efficacy of naturally occurring porphyrins in endothelial cells in vitro and microvasculature in vivo, J. Photochem. Photobiol. B: Biol. 39 (1997) 176–184.

[49] V. Gottfried, R. Davidi, C. Averbuj, S. Kimel, In vivo damage to chorioallantoic membrane blood vessels by porphycene-induced photodynamic therapy, J. Photochem. Photobiol. B: Biol. 30 (1995) 115–121.

[50] M.S. Ismail, C. Dressler, S. Strobele, A. Daskalaki, C. Philipp, H.-P. Berlien, H. Weitzel, M. Liebsch, H. Spielmann, Modulation of 5-ALA-induced PpIX xenofluorescence intensities of a murine tumor and non-tumor tissue cultivated on the chorioallantoic membrane, Lasers Med. Sci. 12 (1997) 218–225.

[51] A. Rueck, N. Akguen, K. Heckelsmiller, G. Beck, F. Genze, R. Steiner, Confocal observations of hydrophilic and lipophilic photosensitizers in endothelial cells, lumen of the vessels, interstitium and tumor cells using the chicken chorioallantoic membrane, Proc. SPIE 3247 (1998) 63–68.

[52] S. Kimel, V. Gottfried, K. Kunzi-Rapp, N. Akguen, H. Schneckenburger, Real time fluorescence microscopy monitoring of porphyrin biodistribution, Proc. SPIE 2628 (1996) 69–76.

[53] S. Koop, I.C. MacDonald, K. Luzzi, E.E. Schmidt, V.L. Morris, M. Grattan, R. Khokha, A.F. Chambers, A.C. Groom, Fate of melanoma

cells entering the microcirculation: over 80% survive and extravasate, Cancer Res. 55 (1995) 2520–2523.

[54] M.J. Hammer-Wilson, L. Akian, S. Kimel, M.W. Berns, unpublished results, 1995.

[55] A. Fuchs, E.S. Lindenbaum, The two- and three-dimensional structure of the microcirculation of the chick chorioallantoic membrane, Acta Anat. 131 (1988) 271–275.

[56] D.O. DeFouw, V.J. Rizzo, R. Steinfeld, R.N. Feinberg, Mapping of the microcirculation in the chick chorioallantoic membrane during normal angiogenesis, Microvascualar Res. 38 (1989) 136–147.

[57] S. Kimel, L.O. Svaasand, M. Hammer-Wilson, M.J. Schell, T.E. Milner, J.S. Nelson, M.W. Berns, Differential vascular response to laser photothermolysis, J. Invest. Derm. 103 (1994) 693–700.

[58] G.S. Rose, L.M. Tocco, G.A. Granger, P.J. DiSaia, T.C. Hamilton, A.D. Santin, J.C. Hiserodt, Development and characterization of a clinically useful animal model of epithelial ovarian cancer in the Fischer 344 rat, Am. J. Obstet. Gynecol. 175 (1996) 593–599.

[59] J.R. Testa, L.A. Getts, H. Salazar, Z. Liu, L.M. Handel, A.K. Godwin, T.C. Hamilton, Spontaneous transformation of rat ovarian surface epithelial cell resulting in well to poorly differentiated tumors with a parallel range of cytogenetic complexity, Cancer Res. 54 (1994) 2778–2784.

[60] A.L. Romanoff, A.J. Romanoff, Biochemistry of the Avian Embryo: a Quantitative Analysis of Prenatal Development, Interscience Publishers, New York, 1967.

[61] S.L. Gibson, J.J. Havens, T.H. Foster, R. Hilf, Time-dependent intracellular accumulation of delta-aminolevulinic acid, induction of porphyrin synthesis and subsequent phototoxicity, Photochem. Photobiol. 65 (1997) 416–421.